

Extended Progress Variable and Mixture Fraction Model for Turbulent Premixed Combustion

Y.Y. Wu and C.K. Chan

Abstract—A approach combining a progress variable and a mixture fraction transport equation is used to describe a turbulent premixed flame with non-uniform equivalence ratio, caused by lateral entrainment of air. The equations are solved using a projection-based fractional step method for low-Mach number flow in a large eddy simulation (LES) framework. The numerical method with a simply extended model is applied to simulate a slot Bunsen flame in two dimensions. The computed mean flame front is comparable to that of experiment and 3D computation using detailed chemical kinetics. The present numerical simulation can also well predict the flame height and the global turbulent flame speed. The computed flame surface density profiles match with those of the experiment.

Index Terms—progress variable, mixture fraction, large eddy simulation, non-uniform equivalence ratio.

I. INTRODUCTION

Aimed to increase efficiency and minimize pollutant emission, turbulent premixed flames are practically important. Many models have been developed for premixed turbulent combustion with uniform equivalence ratio. However, this kind of cases does not often happen in reality and in experiment. According to Prasad et al. [12], spatial and temporal variations in equivalence ratio cannot be avoided in practical combustion, which may be caused by heat losses, or mixing with dilution flows of different enthalpy.

Many laboratory turbulent premixed flames are applied to further understand the interaction of turbulent and flame front, such as turbulent V-flame [1]-[2], swirl-stabilized flame [10], and slot Bunsen flame [3], [15]. Coflow is often used to control the shear layers that form around the fuel/air mixture downstream the inflow. Then turbulent flames do not always burn a homogeneous premixed fuel/air mixture because equivalence ratio varies according to mixing between the main fuel/air inflow and the coflow.

A single scalar of progress variable cannot describe this kind of problems completely because the progress variable is based on uniform equivalence ratio. Additionally a mixture fraction equation is employed to describe the variation of fuel/air mixture. Scalar dissipation term will emerge in the

progress variable equation when a progress variable and a mixture fraction are applied together to describe premixed flames with non-constant equivalence ratio. The term will disappear only for homogenous premixed flames. In many simulations of turbulent premixed flames considering varying equivalence ratio, the term is ignored [12].

In this paper, a simply extended model combining progress variable and mixture fraction is used to describe turbulent premixed flame with varying equivalence ratio in mixing layer. And large eddy simulation of a slot Bunsen flame [15] is used to validate the numerical method with the extended model. In LES method, large scale turbulence is solved directly whereas small scale turbulence is modeled. The simplest LES approach is to use no subgrid scales (SGS) [16]. In the simulation, LES method with a dynamic subgrid model is applied. The flame front is followed by applying a progress variable equation. Additionally a mixture fraction equation is employed to describe the variation of equivalence ratio due to the mixing between fuel/air mixture inflow and coflow. A projection-based fractional step method is employed to numerically solve the equations.

II. BASIC EQUATIONS

With a simple global reaction rate, premixed combustion can be presented by a reactant mass fraction $Y_F(\vec{x}, t)$, which is described by the following equation

$$\frac{\partial(\rho Y_F)}{\partial t} + \nabla \cdot (\rho \vec{u} Y_F) = \nabla \cdot (\rho D \nabla Y_F) - \dot{\omega}_F \quad (1)$$

where $\rho, \vec{u}, \dot{\omega}_F, D, t$ are density, velocity vector, fuel reaction rate, molecular diffusivity, and time respectively. For premixed combustion with varying equivalence ratio, additional scalar variable of mixture fraction $Z(\vec{x}, t)$ is needed. The transport equation of mixture fraction is such as

$$\frac{\partial(\rho Z)}{\partial t} + \nabla \cdot (\rho \vec{u} Z) = \nabla \cdot (\rho D \nabla Z) \quad (2)$$

The above two equations can be combined to applied in whichever premixed, partially premixed, or nonpremixed flames [14].

In the case of simple global reaction rate, progress variable $c(\vec{x}, t)$ is often used instead of $Y_F(\vec{x}, t)$ for convenience. In the thin premixed flame, progress variable changes from zero to unity. With progress variable and mixture fraction, lean reactant mass fraction can be defined by

Manuscript received March 17, 2010. This work was supported by a studentship of The Hong Kong Polytechnic University

Y.Y. Wu is with Department of Applied Mathematics, The Hong Kong Polytechnic University, Hong Kong (e-mail: www.yingyan@polyu.edu.hk).

C.K. Chan is with Department of Applied Mathematics, The Hong Kong Polytechnic University, Hong Kong (phone: 852-27666919; Fax: 852-23344377; e-mail: ck.chan@polyu.edu.hk).

$Y_F(\bar{x}, t) = Y_F [c(\bar{x}, t), Z(\bar{x}, t)]$. And for the premixed combustion with coflow of air or pilot product, following equation can be applied to express lean reactant mass fraction $Y_F(\bar{x}, t) = Y_\phi \cdot Z(\bar{x}, t) \cdot [1 - c(\bar{x}, t)]$ (3)

In the unburnt reactants $Z=1$ and $c=0$, whereas in the burnt product $Z=0$ and $c=1$. Y_ϕ is the mass fraction of fuel in the main fuel/air mixture inflow.

When equation (3) is used to replace mass fraction $Y_F(\bar{x}, t)$ in (1), additional term related to $Z(\bar{x}, t)$ will appear on the right hand of progress variable equation.

$$\frac{\partial(\rho c)}{\partial t} + \nabla \cdot (\rho \bar{u} c) = \nabla \cdot (\rho D \nabla c) + \dot{\omega}_F / (Y_\phi Z) + \frac{2\rho D}{Z} \nabla Z \cdot \nabla c \quad (4)$$

For homogenous premixed combustion $Z(\bar{x}, t) = 1$, and equation (4) reduces to traditional progress variable equation for premixed combustion

$$\frac{\partial(\rho c)}{\partial t} + \nabla \cdot (\rho \bar{u} c) = \nabla \cdot (\rho D \nabla c) + \dot{\omega}_F / Y_\phi \quad (5)$$

where the two terms on right hand side can be combined to be expressed by a formulation of flame surface density $\rho_u S_L \Sigma$. ρ_u is the density of unburnt reactant, S_L is the laminar flame speed, and Σ denotes the flame surface density.

For cases with mixing layer between main fuel/air flow and coflow, the equivalence ratio varies. In mixing layer, laminar flame speed S_L and burnt temperature T_b should change according to the variation of equivalence ratio. The dependence of the scalar field on mixture fraction is taken into account. The third term on right hand side of (4) is also ignored because its source of the diffusion term in (1) is relatively small. The model is extended to consider varying equivalent ratio with mixture fraction such that

$$\frac{\partial(\rho c)}{\partial t} + \nabla \cdot (\rho \bar{u} c) = \rho_u S_d \Sigma \quad (6)$$

where $S_d = S_d(\phi, Z) = S_L \left(\frac{\phi_{local}}{\phi_R} \right)^\gamma$ is the local flame speed,

S_L is the laminar flame speed for reactant with equivalence ratio ϕ_R of main fuel/air mixture, ϕ_{local} is local equivalence ratio, γ is a variable related to the local mixture fraction and is similar to the function proposed by Prasad et al. [19]. Equivalence ratio of $\phi_{min} = 0.5$ corresponds to the lean extinction limit in mixing layer.

With assumption of low-Mach number flow and filtering process of large eddy simulation, non-dimensional governing equations can be obtained as

$$\frac{\partial \bar{\rho}}{\partial t} + \frac{\partial(\bar{\rho} \bar{u}_j)}{\partial x_j} = 0 \quad (7)$$

$$\frac{\partial(\bar{\rho} u_i)}{\partial t} + \frac{\partial(\bar{\rho} \bar{u}_i \bar{u}_j)}{\partial x_j} = -\frac{\partial p'}{\partial x_i} + \frac{\partial m_{ij}}{\partial x_j} \quad (8)$$

$$\frac{\partial(\bar{\rho} \bar{Z})}{\partial t} + \frac{\partial(\bar{\rho} \bar{u}_j \bar{Z})}{\partial x_j} + \frac{\partial[\bar{\rho}(\bar{u}_j z - \bar{u}_j \bar{Z})]}{\partial x_j} = \nabla \cdot (\bar{\rho} \bar{D} \nabla \bar{Z}) \quad (9)$$

$$\frac{\partial(\bar{\rho} \bar{c})}{\partial t} + \frac{\partial(\bar{\rho} \bar{u}_j \bar{c})}{\partial x_j} + \frac{\partial[\bar{\rho}(\bar{u}_j c - \bar{u}_j \bar{c})]}{\partial x_j} = \overline{\rho_u S_d \Sigma} = \rho_u S_d \Sigma \quad (10)$$

where $\bar{\rho}, \bar{u}, p', \bar{Z}, \bar{c}$ denote average density, filtered velocity, pressure fluctuation, filter mixture fraction, and filtered progress variable respectively.

$$m_{ij} = \mu^+ \left(\frac{\partial \bar{u}_i}{\partial x_j} + \frac{\partial \bar{u}_j}{\partial x_i} - \frac{2}{3} \delta_{ij} \frac{\partial \bar{u}_k}{\partial x_k} \right) \quad \text{and} \quad \mu^+ = \mu_t + \mu / \text{Re}$$

with turbulent viscosity $\mu_t = \bar{\rho} C \Delta^2 (2 \bar{S}_{kl} \bar{S}_{kl})^{1/2}$ and filtered

strain rate tensor $\bar{S}_{kl} = \frac{1}{2} \left(\frac{\partial \bar{u}_k}{\partial x_l} + \frac{\partial \bar{u}_l}{\partial x_k} \right)$. μ is dynamic

viscosity, Re is Reynolds number of the flow, and δ_{ij} is Kronecker delta function. C is a model parameter obtained by the dynamic model of Germano et al. [18].

The unclosed transport fluxes in mixture fraction equation and c-equation are modeled with simple gradient expressions.

A flame surface density (FSD) model is used to determine the term on the right hand side of progress variable equation. Based on curvature of the filtered progress variable, flame surface density Σ is computed using a new model proposed by Knikker et al. [20]. The flame surface density is decomposed into a resolved and an unresolved contribution such that

$$\Sigma = |\nabla \bar{c}| + \kappa |\overline{\nabla \cdot N}| M(\bar{c}) \quad (11)$$

where κ is a non-dimensional model constant, $N = \nabla \bar{c} / |\nabla \bar{c}|$ is the unit normal vector normal to iso-contours of the filtered progress variable and M is a masking function to avoid undesired contributions in regions far away from the flame front.

III. NUMERICAL METHODS

For incompressible flows, projection-based fractional step method is an efficient discretization strategy. For low-Mach number reaction flows, projection-based fractional step methods [11], [17], [21]-[23] and the generalized projection approach based on Helmholtz-Hodge decomposing theory [4]-[5] both have successful applications.

With projection-based fractional step method, momentum equation is solved in two parts. Firstly, momentum equations are integrated assuming constant pressure. The pressure fluctuation $p'(\bar{x}, t)$ is then determined before performing the second integration step. Velocities are corrected subsequently according to pressure fluctuation gradients. The corresponding equations are

$$\begin{cases} (\bar{\rho} \bar{u}_i)^* = (\bar{\rho} \bar{u}_i)^n + \Delta t \left[-\frac{\partial(\bar{\rho} \bar{u}_i \bar{u}_j)}{\partial x_j} + \frac{\partial m_{ij}}{\partial x_j} \right] \\ (\bar{\rho} \bar{u}_i)^{n+1} = (\bar{\rho} \bar{u}_i)^* + \Delta t \left[-\frac{\partial p'}{\partial x_i} \right]. \end{cases} \quad (12)$$

The pressure fluctuation is determined by a Poisson equation for $p'(\bar{x}, t)$. This is obtained by taking divergence of the second equation of (12) and being introduced into continuity equation to estimate $\nabla \cdot (\bar{\rho} \bar{u})^n$. The Poisson equation is such as

$$\nabla^2 p' = \frac{1}{\Delta t} \left[(\partial_t \bar{\rho})^{n+1} + \nabla \cdot (\bar{\rho} \bar{u})^* \right] \quad (13)$$

The density variation term $(\partial_t \bar{\rho})^{n+1}$ is included above to eliminate dilatation caused by heat release.

For spacial discretization, staggered grid is employed. A second order upwind finite difference method and a second order central finite difference method are separately used for the convection and diffusion terms. For temporal discretization, a third order Runge-Kutta method is applied to implement time integration.

IV. RESULTS AND DISCUSSIONS

The numerical method with the simply extended model is applied to simulate the turbulent reactive flow field of a slot Bunsen flame. The computation parameters are based on experiments of Filatyev et al. [15]. The slot burner was composed of three rectangular burners: a central burner and two side burners. For all three burners, stoichiometric methane-air mixtures were supplied. The central burner produced Bunsen flame of interest with flat flames from side burners, where hot products flowed at a velocity to match the velocity after Bunsen flame [3].

In experiment, mean properties of the slot Bunsen flames are 2D. In present work, one case of the experimental flames (case 3b) is numerically simulated in two dimensions. For central fuel/air mixture inflow, the dimension is 25 mm and the inflow velocity is mean velocity of 3m/s superimposed with 10% turbulent fluctuation. For side burners, the inflow is hot combustion products in uniform velocity of 7m/s. Reactant is methane-air mixture (CH₄/air) with equivalence ratio of 1.0. Density ratio of stoichiometric reactant to product is given by $\rho_u/\rho_b = 7.47$ and laminar burning speed is taken as $S_L = 0.38 m s^{-1}$. The computational domain is $[-37.5, 37.5]mm \times [0, 100]mm$ and statistical results are obtained by averaging the instantaneous values over 10,000 time steps.

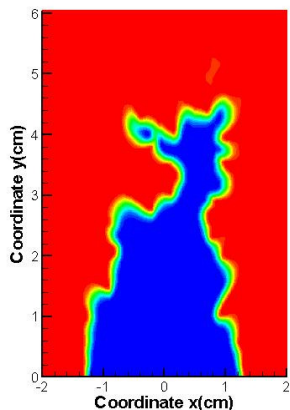


Fig.1 Instantaneous computed slot Bunsen flame

Fig.1 shows an instantaneous computed slot Bunsen flame. The flame front is described by progress variable. In fig.2, the mean flame front is presented by progress variable contour of 0.1-0.9. (a) is from experiment of Filatyev et al. [15] and (b) is from 3D simulation of Bell et al. [3] considering detailed chemical kinetics. (c) presents 2D simulation result. All the average flame heights from experiment and simulations are

about 4cm. The flame front shape of simulations and experiment are very similar except just near the burner exit, where the flame fronts of experiment is more vertical. It may be caused by diversity of turbulent inflow. The downstream flame brush is much thicker than that near the exit. And the downstream mean flame thickness of turbulence is much larger than that of related laminar flame.

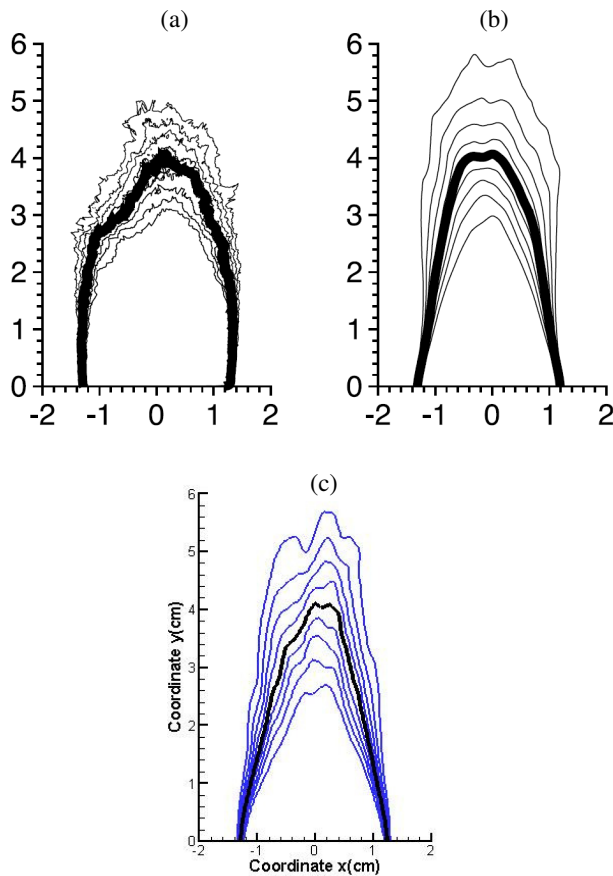


Fig.2 Mean flame front described by progress variable contours of 0.1-0.9 (a) Experiment (b) Simulation result of Bell et al. (c) Present simulation

Fig. 3 contrastively shows the mean axial velocity of present simulation and experiment. The difference may be also induced by turbulent inflow discrepancy.

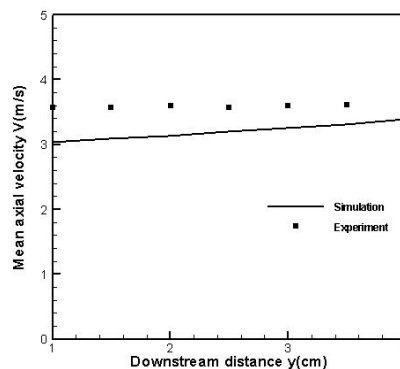


Fig.3 Mean axial velocity along the burner centerline

The mass of reactants mixture entering the center burner per second is $\dot{m}_R = \rho_R L_D \tilde{V}_0 L_h$, and L_D is the length of center burner, L_h is the length along spread direction, \tilde{V}_0 is the mean inflow axial velocity. According to experiment, there is no fuel escape from the burner, the reactants mixture consumed per second can be obtained by mass conservation $\dot{m}_R = \rho_R \bar{S}_T \bar{L}_{0.5} L_h$. $\bar{L}_{0.5}$ is the length of flame front measured from mean progress variable contour $\tilde{c} = 0.5$. So the average global turbulent flame speed is $\bar{S}_T = \dot{m}_R / (\rho_R \bar{L}_{0.5} L_h) = L_D \tilde{V}_0 / \bar{L}_{0.5} \approx 2.3 S_L$. The related quantity of experiment is $\bar{S}_T \approx 2.55 S_L$.

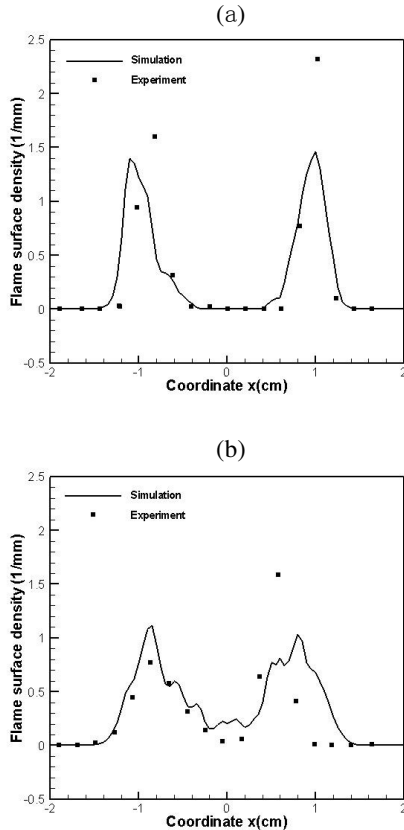


Fig.4 Mean flame surface density at (a) $y=2.8\text{cm}$ and (b) $y=5\text{cm}$

Fig.4 depicts mean flame surface density at $y=2.8\text{cm}$ and $y=5\text{cm}$. Line shows the computed results and dot presents the experiment results. The figure does not show symmetry. In experiment, it is due to nonuniform flow in the burner internal flow field [15]. In numerical simulation, it may be generated by random inflow velocity fluctuations. However, the results of simulation and experiment agree well.

V. CONCLUSION

In practical and experimental combustions, spatial and temporal variations in equivalence ratio often happen. It may be caused by heat losses, or mixing with dilution flows of different enthalpy. In this paper, combined progress variable and mixture fraction with a simply extended model is used to

describe turbulent premixed flames with varying equivalence ratio in mixing layer. Large eddy simulation of a slot Bunsen flame is performed. Compared with experiment and 3D computation with detailed chemical kinetics, present numerical method with extended model well predicts mean flame front, flame height, and global turbulent flame speed. The computed flame surface density profiles also match with those of the experiment. The results indicate that present numerical method can reasonably simulate turbulent premixed flame with varying equivalence ratio, which has two dimensional mean properties. In future work, we will try to explore the extended model in three dimensions.

ACKNOWLEDGMENT

The authors wish to thank Dr. Karl-Johan Nogenmyr for his useful discussion and constructively suggestion.

REFERENCES

- [1] R.K. Cheng, Conditional sampling of turbulence intensities and Reynolds stress in premixed turbulent flames, *Combustion Science and Technology*, 41(1984)109-142.
- [2] J.B. Bell, M.S. Day, I.G. Shepherd, M. Johnson, R.K. Cheng, J.F. Grcar, V.E. Becker and M.J. Lijewski, Numerical simulation of a laboratory-scale turbulent V-flame. Lawrence Berkeley National Laboratory report LBNL-54198-Journal.
- [3] J.B. Bell, M.S. Day, J.F. Grcar, M.J. Lijewski, J.F. Driscoll, and S.A. Filatyev, Numerical simulation of a laboratory-scale turbulent slot flame, *Proc. Combust Inst.* 31 (2007) 1299-1307.
- [4] J.B. Bell, M.S. Day, J.F. Grcar, M.J. Lijewski, M. Johnson, R.K. Cheng, I.G. Shepherd, Numerical simulation of a premixed turbulent V-flame. *Int. Coll. Dyn. Explo. React. Sys.*, Japan, 2003.
- [5] J.B. Bell, M.S. Day, J.F. Grcar, M.J. Lijewski, A computational study of equivalence ratio effects in turbulent, premixed Methane-Air flame. *Proc. ECCOMAS-CFD, the Netherlands*, 2006.
- [6] C.K. Chan, K.S. Lau, B.L. Zhang, Simulation of a premixed turbulent flame with the discrete vortex method. *Int. J. Numer. Meth. Engng.* 48 (2000) 613-627.
- [7] C.K. Chan, H.Y. Wang, H.Y. Tang, Effect of intense turbulence on turbulent premixed V-flame. *Int. J. Eng. Sci.* 41 (2003) 903-916.
- [8] C.K. Chan, B. Stewart, C.W. Leung, Numerical Simulation of Premixed V-Flame, *Proc. Int. Conf. Mech. Eng.* 2007, 1317-1321.
- [9] T. Poinsot, D. Veynante, *Theoretical and Numerical Combustion*. 2001.
- [10] K.-J. Nogenmyr, P. Petersson, X.S. Bai, A. Nauert, J. Olofsson, C. Brachman, H. Seyfried, J. Zetterberg, Z.S. Li, M. Richter, A. Dreizler, M. Linne and M. Alden, Large eddy simulation and experiments of stratified lean premixed methane/air turbulent flames, *Proc. Combust Inst.* 31(2007)1467-1475.
- [11] Y. Liu, K.S. Lau, C.K. Chan, Y.C. Guo, W.Y. Lin, Structures of scalar transport in 2D transitional jet diffusion flames by LES, *Int. J. Heat Mass Tran.* 46(2003)841-3851.
- [12] R. O. S. Prasad, R. N. Paul, Y. R. Sivathanu, and J. P. Gore, An evaluation of combined flame surface density and mixture fraction models for nonisenthalpic premixed turbulent flames, *Combust. Flame.* 117(1999)514-528.
- [13] P. Bigot, M. Champion and D. Garréon-Bruguères, Modeling a turbulent reactive flow with variable equivalence ratio: Application to a flame stabilized by a two-dimensional sudden expansion, *Combust. Sci. and Tech.* 158(2000)299-320.
- [14] K. Bray, P. Domingo and L. Vervisch, Role of the progress variable in models for partially premixed turbulent combustion, *Combust. Flame.* 141(2005)431-437.
- [15] S.A. Filatyev, J.F. Driscoll, C.D. Carter, and J.M. Donbar, Measured properties of turbulent premixed flames for model assessment, including burning velocities, stretch rates, and surface densities, *Combust. Flame.* 141(2005)1-21.
- [16] J. Janicka, A. Sadiki, Large eddy simulation of turbulent combustion systems. *Proc. Combust Inst.* 30 (2005) 537-547.
- [17] J. de Charentenay, D. Thévenin, B. Zamuner, Comparison of direct numerical simulation of turbulent flames using compressible or low-Mach number formulations, *Int. J. Numer. Meth. Fl.* 39 (2002) 497-515.

- [18] M. Germano, U. Poinmelli, P. Moin, W.H. Cabot, A dynamic subgrid-scale eddy viscosity model. *Phys. Fluids*, 3(1991)1760-1765.
- [19] R. O. Prasad, R. N. Paul, Y. R. Sivathanu, J. P. Gore, An evaluation of combustion flame surface density and mixture fraction models for nonisenthalpic premixed turbulent flames, *Combust. Flame*. 117 (1999) 514-528.
- [20] R. Knikker, D. Veynante, J.C. Rolon, C. Meneveau, Planar laser-induced fluorescence in a turbulent premixed flame to analyze large eddy simulation models, *Proc. Int. Symp. Turb., Heat and Mass Tran.*, Lisbon, 2000.
- [21] B. Lessani, M.V. Papalexandris, Time-accurate calculation of variable density flows with strong temperature gradients and combustion. *J. Comput. Phys.* 212 (2006) 218-246.
- [22] H.N. Najm, P.S. Wyckoff, O.M. Knio, A semi-implicit numerical scheme for reacting flow: I. Stiff Chemistry. *J. Comput. Phys.* 143 (1998) 381-402.
- [23] F. Nicoud, Conservative high-order finite-difference schemes for low-Mach number flows. *J. Comput. Phys.* 158 (2000) 71-97.
- [24] H. Lahjaily, M. Champion, D. Karmed and P. Bruel, Introduction of Dilution in the BML Model: Application to a stagnating turbulent flame, *Combust. Sci. and Tech.* 135(1998)153-173.